HHS Public Access

Author manuscript

Comput Biol Med. Author manuscript; available in PMC 2016 October 01.

Published in final edited form as:

Comput Biol Med. 2015 October 1; 65: 200–208. doi:10.1016/j.compbiomed.2015.04.036.

Computational Modeling of Cardiac Optogenetics: Methodology Overview & Review of Findings from Simulations

Patrick M. Boyle[1,*], **Thomas V. Karathanos**[1], **Emilia Entcheva**[2], and **Natalia A. Trayanova**[1]

[1]Institute for Computational Medicine and Department of Biomedical Engineering at Johns Hopkins University, 3400 N Charles St – 316 Hackerman Hall – Baltimore MD 21218 – USA

[2]Department of Biomedical Engineering, Stony Brook University, Stony Brook, NY 11790

Abstract

Cardiac optogenetics is emerging as an exciting new potential avenue to enable spatiotemporally precise control of excitable cells and tissue in the heart with low-energy optical stimuli. This approach involves the expression of exogenous light-sensitive proteins (opsins) in target heart tissue via viral gene or cell delivery. Preliminary experiments in optogenetically-modified cells, tissue, and organisms have made great strides towards demonstrating the feasibility of basic applications, including the use of light stimuli to pace or disrupt reentrant activity. However, it remains unknown whether techniques based on this intriguing technology could be scaled up and used in humans for novel clinical applications, such as pain-free optical defibrillation or dynamic modulation of action potential shape. A key step towards answering such questions is to explore potential optogenetics-based therapies using sophisticated computer simulation tools capable of realistically representing opsin delivery and light stimulation in biophysically detailed, patient-specific models of the human heart. This review provides (1) a detailed overview of the methodological developments necessary to represent optogenetics-based solutions in existing virtual heart platforms and (2) a survey of findings that have been derived from such simulations and a critical assessment of their significance with respect to the progress of the field.

Graphical Abstract

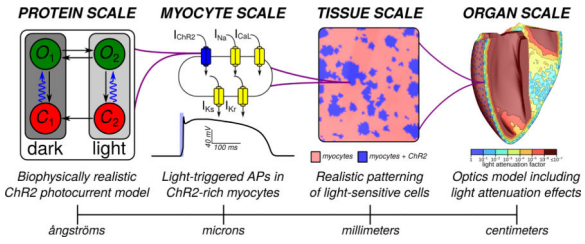

* Corresponding author: PM Boyle Phone: 443-838-1203, Fax: 410-516-5294, pmjboyle@jhu.edu.

Conflicts of Interest

The authors hereby declare no financial or personal relationships with other people or organizations that could inappropriately bias this work.

Introduction

Cardiac optogenetics is an exciting new field in which cells in the heart are genetically modified to express light-sensitive proteins (opsins) so that low-energy light can be used to induce transmembrane current, providing a means for electrophysiological control (1,2). Many different types of opsins exist, including ionic channels and pumps that produce different types of membrane current (i.e., depolarizing or hyperpolarizing) when illuminated with light in a particular wavelength range (3-8); this rich diversity means that optogenetics enables numerous useful applications in opsin-expressing tissue, including eliciting or suppressing action potentials (APs) with exquisite spatiotemporal specificity. Thus far, this versatile approach has been implemented using transgenic animals (with global cardiac expression) and in cells, tissue, and organs that have been light sensitized by gene or cell delivery (9-13). Beyond its irrefutable appeal as a basic science tool, it remains to be seen whether optogenetics-based solutions may provide an alternative to electrotherapy to treat cardiac arrhythmias (14,15). Computer modeling provides an avenue to narrow the scope of experimental investigations by helping to pinpoint which light-based therapy innovations are most likely to make a difference in the clinic. The aim of this review is to summarize the work that has been done so far towards virtual cardiac optogenetics, i.e. the incorporation of optogenetic tools in realistic simulations of the heart. First, we provide a comprehensive overview of the methodological approach for integrating new features at the sub-cellular (protein), cellular, tissue, and organ scales of biophysically-detailed cardiac models; then, we highlight interesting and relevant findings that have emerged from simulations of cardiac optogenetics to date.

Methodology Overview

Simulations conducted in detailed models of the heart (ventricular, atrial, or whole-heart) are increasingly recognized as an essential aspect of the investigation of cardiac disease (16-19), with applications ranging from mechanistic analysis of rhythm disorders (20-29) or pump dysfunction (30-33) to the development of novel therapeutic methodologies (34-36). Excitingly, the emergence of models reconstructed from medical images (obtained via magnetic resonance, computed tomography, etc.), which incorporate patient-specific detail about cardiac geometry and structural remodeling, has opened up new avenues for translating results from simulations into insights relevant to clinical applications (37-43). Since optogenetics has emerged at a time when such a rich and robust set of tools for cardiac computational modeling exists, there is great enthusiasm to discover what might be learned about this exciting new technology if it can be explored in biophysically-detailed models of the heart (1,14,15); to achieve this goal, new methodologies have been developed to represent light sensitization and optical stimulation at multiple spatial scales (44), as summarized in Fig. 1. At the protein scale (I), the light- and voltage-sensitive electrical properties of opsins expressed in the sarcolemma are represented; at the cell scale (II), the integration of opsins in individual myocytes or exogenous donor cells is modeled; at the tissue scale (III), the heterogeneous spatial distribution of opsin-expressing cells resulting from light sensitization must be represented; finally, at the organ scale (IV), it is necessary to capture the application of optical stimuli to the heart, taking into account light-matter interactions resulting in photon scattering and light attenuation. This section provides a

detailed review of different methodologies that have been devised, either in the context of cardiac optogenetics or for other multiscale heart modeling studies.

Modeling Cardiac Optogenetics at the Protein Scale—The first step towards multiscale simulation of cardiac optogenetics is the development of accurate models of the light- and voltage-dependent electrophysiological behavior of opsins. Initial efforts in this direction have focused on the algal blue light-sensitive protein channelrhodopsin-2 (ChR2), the most widely used excitatory opsin in optogenetics research. ChR2 forms a light-sensitive cation channel that is permeable to H^+, Na^+, K^+, and Ca^{2+}, with a reversal potential of approximately 0 mV (3). Analysis of spectral characteristics revealed that ChR2 energy absorption is maximal for light with a wavelength of approximately 480 nm (45). Hegemann et al. formulated the first mathematical description of the ChR2 photocycle (46), proposing a Markov model with states representing open, closed, and refractory channel configurations; a rapid closed-to-open transition in the presence of blue light was found to be necessary to achieve a simulated ChR2 current (I_{ChR2}) consistent with experimental measurements. Based on experiments in voltage-clamped ChR2-expressing cells revealing I_{ChR2} with a distinct a peak-and-plateau morphology, potentiated by the irradiance of the optical stimulus, it was inferred that a model with at least four states (including a second open state associated with a refractory light-adapted channel configuration) was required to fully reproduce the photosensitive properties of ChR2 (45,47).

Recent efforts by Williams et al. (48) led to characterization of both light- and voltage-sensitive properties of ChR2 photocurrent and its operation in cardiomyocytes. Based on experimental data, an extended version of the four-state model by Nikolic et al. (47) was put forward, that includes voltage rectification and voltage dependence of kinetic parameters. The inclusion of an empirical scaling function to represent ChR2's voltage rectification was found to be essential in accurately reproducing the behavior of I_{ChR2} during the different phases (upstroke, notch, plateau, repolarization) of light-triggered cardiac action potentials (APs). Experimental validation was enabled by an “optical AP clamp” to extract the I_{ChR2} waveform during light-triggered cardiac AP (48,49). This approach involves measuring the total membrane current in a ChR2-expressing cell with membrane voltage clamped to a specific AP morphology and recreation of the optical stimulus used to trigger the AP; by comparing currents in the presence and absence of illumination, the dynamic I_{ChR2} during the AP can be extracted.

Fig. 2A shows photocurrent traces in response to 5 blue light pulses of different intensity for the ChR2 model by Williams et al. in cells clamped to resting V_m = –80 mV. Fig. 2B shows the response to both electrical and optogenetics-based stimuli in a simulated cardiomyocyte (50): first, two electrically-paced APs; then, two APs prolonged by the application of strong light stimuli during the plateau phase (200 and 400 ms long, each delivered 100 ms after the AP-triggering electrical stimulus); finally, four APs that are triggered purely by light pulses of different durations (10, 50, 100, and 400 ms).

In addition to ChR2, other opsins have been studied, but few have been characterized mathematically. Popular inhibitory opsins include the light-sensitive chloride pump halorhodopsin (NpHR) and the proton pump Archaerhodopsin-T (ArchT). In contrast to

ChR2, illumination of NpHR or ArchT results in an outward (repolarizing) current that has been used to silence electrical activation in spontaneously activating cardiac cells (11,12,51). Nikolic et al. developed a three-state model of NpHR (open, closed, desensitized) and showed that light stimulation of a simulated NpHR-expressing neuron silenced excitation, even in the presence of a driving stimuli (52). Fig. 2C shows NpHR current (I_{NpHR}) profiles in response to orange light pulses; the model used here is an original implementation by the authors of this paper, adapted from the Nikolic et al. version (52) with some parameters calibrated to match photocurrent values recorded in NpHR-expressing myocyte (51), as summarized in Table 1. Consistent with experimental observations (6), the model produced peak and plateau I_{NpHR} values that were much smaller in magnitude than I_{ChR2} for light stimuli with the same E_e values. The behavior of the photocurrent produced by NpHR and ArchT is qualitatively similar (53), thus lessons learned from computational studies with a simple generic model of an inhibitory opsin are relevant to both. Fig. 2D shows that when the I_{NpHR} model was incorporated in a cardiomyocyte model (50), application of orange light inhibited the initiation of APs by electrical stimuli. However, it must be noted that electrical stimuli in this case were only 35% higher than the excitation threshold (32.4 vs 24 $\mu A/cm^2$); when stronger electrical pulses were applied, hyperpolarizing current from NpHR failed to prevent AP initiation, although AP duration was abbreviated. This is consistent with in vitro experiments on NpHR-expressing myocytes, in which illumination could reliably shorten APs but rarely suppressed them completely (51). In general, the photocurrents produced by the first generation inhibitory opsins (pumps) are insufficient to reliably counter and completely halt cardiac activity at the tissue level without having to employing high irradiances that may produce heating, as explained in Supplementary Material published by Williams et al. (48).

Future efforts in this field should include the development of detailed biophysical models of bioengineered variants of ChR2 and other opsins with desirable characteristics for therapeutic applications in the heart. For example, CatCh (54) has increased permeability to Ca^{2+} and has been used in vitro for termination of arrhythmogenic reentry in neonatal rat atrial myocyte monolayers (55); other notable variants are ChRonos (56) with accelerated channel kinetics, and ChRimson (56) or ReaChR (57), a red-shifted mutant better suited for in vivo applications due to better light penetration compared to the blue light used to excite ChR2. Alternatively, computational efforts in this area can be used to propose new features for optical actuators to be engineered in the context of organ-scale cardiac applications.

Modeling Cardiac Optogenetics at the Myocyte Scale—At the myocyte level, it is necessary to represent the different approaches that have been used to inscribe light sensitivity. From the modeling perspective, these can be classified into two broadly defined paradigms, both of which are discussed below: (1) direct expression of opsins in cardiac myocytes and (2) electrical coupling of exogenous opsin-expressing cells (i.e., donor cells) to myocytes (i.e., host cells). The first approach comprises both gene delivery (GD), which uses viral vectors to light-sensitize cardiomyocytes directly in vitro (51,55,58,59) or in vivo (13), and the creation of transgenic cells, tissue, and organisms from opsin-expressing embryonic stem cells (9,12,60-62). From a computational standpoint, this paradigm is represented in models of transduced cells by adding the opsin-mediated current in parallel to

endogenous membrane currents (due to ion channels, pumps, and exchangers) of the cardiomyocyte. This approach has been used to simulate the light sensitization process in a variety of cell types (atrial, ventricular, specialized conduction system, etc.) for numerous different species (human, canine, rabbit, etc.) (44,48,49,61).

The second approach, a cell delivery (CD) method, involves the use of dedicated opsin-rich donor cells; these cells are then co-cultured with host cardiac cells or injected into the beating heart muscle and, if coupled to the host cells, provide light sensitivity. The proof-of-concept in vitro work for CD involving optogenetic transgenes was carried out using ChR2-transfected human embryonic kidney (HEK-293) cells (i.e., somatic cells) (10). These were shown to form electrically coupled “tandem cell units” (TCUs) with neonatal rat ventricular myocytes, resulting in a light-excitable syncytium. Optical mapping confirmed light-paced excitation waves in the resultant hybrid tissue from co-culturing of these two cell types (10). Subsequent work by Nussinovitch et al. applied the CD approach using the NIH3T3 fibroblast cell line expressing either excitatory or inhibitory opsins (11). Computationally, there are two steps involved in the realistic representation of opsin-rich donor cells. First, an appropriate electrophysiological model for the donor cell is chosen and the opsin-mediated current is added in parallel to endogenous donor cell ionic currents. For cardiac applications explored thus far, the use of an electrically passive cell model (i.e., a parallel resistor-capacitor circuit with a fixed resting potential) has proved appropriate for representing inexcitable donor cell types (e.g., HEK-293 or NIH-3T3) (11,44). Modeling should be extended to other donor cell types potentially relevant for CD applications, e.g. cardiac fibroblasts (63) or stem cell derived cardiomyocytes. The second step is to incorporate into the model a representation of the extent of electrical coupling between donor and host cells. This problem must be tackled on a case-by-case basis by incorporating observations from experiments with electrically coupled donor and host cells; for example, Jia et al. used dual-cell patch clamp recordings in light-sensitive TCUs to demonstrate that the minimum coupling conductance between ChR2-rich somatic cells and cardiomyocytes required for CD-mediated optogenetics was approximately 2nS(10).

Modeling Cardiac Optogenetics at the Tissue Scale—Important aspects for modeling at the tissue level is the incorporation of realistic spatial patterns of opsin-expressing cells, resulting from either viral transfection (GD) or donor cell injection (CD). Spatial expression characteristics particular to optogenetics have not been characterized for in vivo applications of gene or cell delivery. Based on experimental data from other transgene applications, it is reasonable to expect that there will be a wide variety of heterogeneous patterns depending on both the moiety of infection (i.e., multiplicity of transduced units) and the method of delivery (i.e., localized versus systemic delivery) (64-66). Although it may be possible to obtain image-based models of transduced cell distribution by segmenting then processing confocal images of flurophore-tagged opsins (10), this methodology could prove extremely tedious and time consuming for whole hearts.

For computational applications, a stochastic algorithm can be used to generate in silico light-sensitive cell spatial distributions that mimic patterns observed for GD and CD studies in vitro (44). This algorithm was originally devised by Comtois et al. (67) to represent different types of fibrosis distributions in 2D models of atrial tissue; Boyle et al. (44) extended the

methodology for use in 3D and proposed its use to represent light-sensitive cell distributions. This algorithm generates spatial patterns by control of two parameters that range from zero to one: density (D) and clustering (C). Within a particular tissue volume defined as the target for light sensitization, elements were deemed opsin-expressing one-by-one until the proportion of light-sensitive tissue by volume was equal to the target value D. Critically, a stochastic process was used to determine whether each new light-sensitive element should be added to an existing cluster of opsin-expressing tissue (with probability C) or if a new cluster should be started at a random location within the target volume. This resulted in a range of spatial distributions of optogenetically-transduced units, including both highly clustered patterns (the expected result of direct myocardial injection (64,65)) and highly diffuse patterns (as anticipated for systemic delivery (66)).

Four unique spatial distributions of opsin-expressing cells in an image-based model of the human left atrium (68,69) are shown in Figs. 3A-D (D = 0.4, C = 0, 0.35, 0.65, and 0.95, respectively). As the C parameter value increases, there was a clear qualitative trend towards aggregation of light-sensitive elements into distinct clusters. Moran's I spatial autocorrelation (70) was calculated for these models and others (with different D values); this metric yields values closer to zero for more diffuse distributions and closer to one for clustered spatial patterns. As shown in Fig. 3E, findings from this quantitative analysis were consistent with the observed effect of the C parameter from Figs. 3A-D, regardless of D value.

Modeling Cardiac Optogenetics at the Organ Scale—The steps necessary for simulating the dynamics of excitation and contraction in biophysically-detailed and anatomically realistic models of the atria (71) and ventricles (17,72) are well known, but additional steps are needed to represent the optical stimuli that would be applied as part of any optogenetics-based treatment methodologies. Recent studies have outlined possible approaches for applying such light stimuli to the beating heart, including miniaturized endoscopic fiber optics-based systems (73), injectable optoelectronics compatible with cardiac tissue (74), and flexible membranes studded with light-emitting diodes (75). Nonetheless, it remains largely unknown how the efficacy of optogenetics-based treatments will be affected by the attenuation of light energy applied to the heart, caused by photon scattering and absorption by tissue and blood (76-79). One approach to model light-tissue interactions is to track the behavior of individual photon packets in heart tissue via Monte Carlo methods (79). This approach results in a highly accurate approximation of the 3D distribution of irradiance resulting from cardiac illumination, including subtle effects such as the sub-surface energy peak caused by photon back-scattering (76); however, it is computationally intense (79) and representation of back-scattering is considered non-essential in the context of cardiac optogenetics (2), since the primary light-related constraint is the fact that opsin-exciting light cannot penetrate very deeply in cardiac tissue. An appropriate and computationally expedient alternative is to approximate model attenuation effects by solving the steady state photon diffusion equation, which assumes homogeneous absorption and isotropic scattering in the cardiac tissue:

$$\mathrm{D}\nabla^2 \mathrm{E}_e\left(\mathbf{r}\right) - \mu_\mathrm{a}\,\mathrm{E}_e\left(\mathbf{r}\right) = -\,\mathrm{w}\left(\mathbf{r}\right)$$

where E_e and w are, respectively, the distributions of irradiance and photon sources at each point r; ∇^2 is the Laplace operator; D is the diffusivity of light in the medium (which depends on absorption and scattering characteristics); and μ_a is the tissue-specific rate of light absorption. Values of the latter two coefficients also depend on the wavelength (λ) of light used to illuminate tissue; nominal values for blue (λ = 488 nm; D = 0.18 mm, μ_a = 0.52 mm^{-1}) and red light (λ = 669 nm; D = 0.34 mm, μ_a = 0.10 mm^{-1}) are known from previous optical experiments (80). In practice, the equation is solved with w = 0 within the tissue and E_e values imposed as a Dirichlet boundary condition on the entire heart surface, with E_e = $E_{e,max}$ at directly-illuminated points (where $E_{e,max}$ is the irradiance of unattenuated light) and E_e = 0 elsewhere on the surface (78). Lastly, for simple optical stimulation configurations (e.g., a single light source), light attenuation can be approximated by an exponential decay (44,78):

$$E_e(\mathbf{r}) = E_{e,max} e^{\frac{d}{\delta}}$$

where d is the distance from point **r** to the nearest illuminated point and $\delta = \sqrt{D/\mu_a}$ is the optical penetration depth (588 μm and 1.84 mm for blue and red light in cardiac tissue, respectively).

Spatial profiles of irradiance are shown for four unique optical stimulation configurations in Fig. 4; these distributions were generated by using a finite element method to solve the steady-state photon diffusion equation (78), as described above. The examples shown here compare blue (Figs. 4A-B) and red light sources (Figs. 4C-D) as well as illumination of the entire epicardium (Figs. 4A,C) versus multiple distributed points (Figs. 4B,D). The differences between these maps highlight the impact of wavelength on light attenuation in cardiac tissue, as evidenced by the difference in E_e values on the endocardial surface of the left ventricular free wall; red light applied epicardially was reduced by 2-3 orders of magnitude, whereas blue light was attenuated to ~10^{-6} of $E_{e,max}$.

Finally, an important aspect of cardiac optogenetics modeling is the ability to estimate the input energy requirements for optical stimuli, which enables a direct comparison of proposed clinical light therapy approaches with existing electrical techniques. Boyle et al. (2) used values reported for single-optrode neural optogenetics applications (74) to derive a straightforward method for approximating the energy requirements for ChR2 excitation with any number of arbitrarily-sized optrodes; they inferred that the input energy required to achieve an irradiance of 10 mW/mm^2 for one second is approximately 208.3 mJ per square millimeter of directly-illuminated tissue.

Insights from Simulations of Cardiac Optogenetics

Effects of Cardiac Cell Type on Energy Required for Optogenetics-Based Stimulation—Cells in different parts of the heart undergo APs with distinct properties, which stem from major differences in the makeup of inward and outward membrane currents. Since optogenetics-based stimulation involves light-induced depolarizing or hyperpolarizing transmembrane stimuli, differential energy requirements are expected for

the optical induction of AP in different cell types given a certain opsin expression rate. Williams et al. (48) simulated the performance of ChR2 alongside the native membrane currents from ion channels, pumps, and exchangers in human ventricular (50), atrial (81), and specialized conduction system cells (i.e., Purkinje fibers) (82). As shown in Fig. 5, these experiments revealed differences between the three cell types in terms of the rheobase and chronaxie value of strength-duration curves; Purkinje fibers were optically excitable with the lowest-energy light stimuli, followed by atrial cells then ventricular myocytes. The authors showed that this effect was attributable to variation in the native ionic currents active during the early stages of the AP, with the inward rectifying potassium current (I_{K1}) playing a particularly prominent role; indeed, when the native I_{K1} formulation for the ventricular model was replaced by the one from the Purkinje fiber model, there was a significant improvement in optical excitability (lower threshold for excitation) in such ventricular myocytes. In a follow-up study (83), the same group demonstrated that, in spite of fundamental differences between the mechanisms of cellular depolarization, the primary determinants of electrical and optical excitability are the same (namely, dynamic variations in cardiomyocyte membrane resistance and inward rectifier current due to intrinsic properties of different cell types).

Optogenetics-Based Cardiac Pacing—Single cell-level factors for optogenetic stimulation, such as those considered by Williams et al. (48), are further compounded by tissue-level (multicellular and coupling) effects in the response of cardiac tissue to light. For instance, in addition to having intrinsically higher excitability due to membrane ion channel composition, Purkinje fibers also experience weaker electrotonic loading effects compared to the well-coupled 3D atrial and ventricular tissues because the cardiac conduction system is organized into a branching network of cable-like bundles (84). Multiscale models using the methodological approach outlined in the first part of this review, implemented by Abilez et al. (61), Wong et al. (85), and Boyle et al. (44), provide further insights on the contribution of such tissue-level phenomena in optogenetic responses. For example, optogenetics-based pacing of ChR2-expressing Purkinje fibers was found to be possible with much lower irradiance levels ($E_e \leq 1.69$ mW/mm^2) compared to analogous stimulation of ventricular sites ($E_e = 6.49$ mW/mm^2) (44).

Other aspects of cardiac optogenetics-based pacing were also tested in such multiscale simulations. Abilez et al. (61) first demonstrated that photocurrent induced in a small island of ChR2-expressing cells (measuring ≥ 0.02 cm^3) would be sufficient to overcome the sink effect imposed by electrical coupling with surrounding non-light-sensitized myocytes. Limitations due to light attenuation effects or non-uniformities in ChR2 spatial pattern (not considered in (61)) were further studied by Boyle et al. (44). The threshold irradiance ($E_{e,thr}$) required for optogenetics-based pacing of cardiac tissue was determined for different delivery modes – direct gene delivery of ChR2 in cardiomyocytes (GD) versus injection of specialized non-excitable ChR2-rich donor cells (CD) - and for different spatial distribution of light-sensitive cells (comparing diffuse versus clustered patterns). For light sensitization via GD, $E_{e,thr}$ depended predominantly on the amount tissue expressing ChR2 (i.e., higher density resulted in lower threshold values); the relationship for CD cases was less straightforward, with the lowest $E_{e,thr}$ values corresponding to spatial distributions that

maximized the interface between electrical sources (opsin-rich donor cells) and sinks (normal myocytes). Understanding such relationships is important in the context of potential in vivo applications of optogenetics-based pacing (13) as non-uniformity of spatial opsin patterns is expected.

The cardiac optogenetics simulation methodology described in the first part of this review is highly versatile and can be used in heart models of arbitrary complexity, simulating diseased stated and different species, and capturing the complex electromechanical response of the heart. Boyle et al. (44) simulated optogenetics-based pacing in a canine model of cardiac electromechanical contraction, within which myofilament shortening was coupled to electrical activation via the intracellular calcium signal at each point in the ventricles (86,87). For the case shown here, 10 optical stimulation sites were chosen at endocardial locations corresponding to Purkinje system endpoints in the left and right ventricles; for each site, cells within a hemispherical tissue volume (3 mm in diameter) were modeled as light-sensitive and uniform endocardial illumination was applied. This resulted in electrical activation (Fig. 6A) and mechanical deformation (Fig. 6B) consistent with normal sinus rhythm, as reflected by the fact that pressure-volume loops corresponded closely to those resulting from electrical stimulation of the His bundle, reassuring of the equivalence of electrical and optogenetic stimulation.

Dynamic Modulation of Atrial Action Potential Duration (APD)—Unlike electrical stimulation, optogenetics-based perturbations, relying on depolarizing and hyperpolarizing currents, provide a finer tool to modulate the morphology of cardiac APs (1,49,51). These features make optogenetic stimulation a potentially unique tool for mitigating deleterious effects of APD-altering pathological conditions. Karathanos et al. (88) illustrated this concept by conducting cell- and organ-scale simulations in human atrial models affected by short QT syndrome (SQTS) (26). This study showed that abnormal APD shortening due to mutant inward rectifier potassium current (I_{K1}), the underlying cause of the SQTS variant in question, could be almost completely eliminated by illuminating ChR2-rich cells with appropriately shaped optical pulses (Fig. 7A). The proposed light-based treatment yielded an AP that was closer in shape and duration to the control case compared to the AP resulting from optimal drug treatment (Figs. 7B,C). Comparable findings were reported by Park et al. in a concurrent in vitro study (51), which elegantly demonstrated the feasibility of optogenetics-based APD lengthening in neonatal rat ventricular myocytes transfected with ChR2. Such cells exhibit action potential morphologies resembling those of atrial cells as in (89), with plateaus at voltages below 0mV permitting the inward flow of ChR2 current and thus APD prolongation; however, in (human) ventricular myocytes APD prolongation via ChR2 is limited (49) due to the rectifying function of ChR2, as revealed computationally. Furthermore, optogenetics-based APD shortening was demonstrated in vitro by using NpHR in neonatal rat myocytes and illuminating with green light (51); future simulations with inhibitory opsins can yield insights relevant to APD modulation and cardioversion.

Analogous simulations exploring APD modulation in organ-scale simulations were conducted to ascertain whether an optogenetics-based approach might be able to mitigate the effects of SQTS in the human atria (88); this would be of therapeutic benefit, since AF is a common complication arising from SQTS (26). Simulations were conducted in an image-

based model of the human left atrium (69,90); under idealized conditions for optogenetics-based treatment (ChR2 expression in 100% of myocytes, no light attenuation), illumination with a similar pulse sequence that restored healthy APD significantly prolonged APs throughout the atria (mean ± standard deviation for control, SQTS, and light-treated SQTS were 250.5±1.5, 137.6±0.9, and 218.4±1.2 ms, respectively). With a more realistic diffuse distribution of opsin-expressing cells throughout the tissue (D = 0.4, C = 0.05; comparable to patterns observed in vivo resulting from GD of ChR2 via systemic injection in mice (13)), the therapy was less effective (APD = 180.7±3.0 ms). Finally, the addition of realistic light attenuation effects almost completely abolished the therapeutic benefit of illumination (APD = 144.8±3.5 ms). This study highlighted the complex nature of optogenetic response at the whole-heart level, and the practical limitations of the technology in its present state, particularly for applications beyond simple localized optical pacing, due to limited capacity to capture deep tissue with shorter-wavelength light. The authors concluded that it might be possible to offset this constraint by using engineered ChR2 variants with higher conductance and/or spectral sensitivity more favorable to deep light penetration (i.e., ChRimson (56) or ReaChR (57)). Such opsins have to offer increased photocurrent and be operational at low-light levels because with red-shifted excitation, potential thermal heating issues become relevant and need to be taken into account (58) – another venue conducive for computational input.

Conclusions

This review summarized the main components necessary for simulating cardiac optogenetics in biophysically detailed multiscale models of the heart (including patient-specific image-based models) and discussed findings and insights obtained by such simulations. Model-based research has the potential to accelerate progress in this fledgling field by (a) providing detailed feasibility assessments for potential organ-scale light-based therapies and (b) identifying critical bottlenecks for scaling up applications from smaller to larger-scale experimental preparations (e.g., the severe limitations imposed by light attenuation in the context of optogenetics-based APD modulation). Notably, the fact that optogenetics has emerged at a time when robust and flexible tools for conducting realistic organ-scale simulations of the heart already exist provides a unique opportunity. In addition to aiding in data analysis and interpretation, computational modeling in cardiac optogenetics has the potential to provide guidance in the development of new optogenetic tools by virtual pre-testing thereby helping to focus the experimental pursuits on the most promising optogenetic solutions.

Acknowledgements

The authors wish to thank Ms. Aleks Klimas for illuminating discussions regarding intracardiac light delivery and cell heating effects and Dr. Dafang Wang for helpful advice regarding the implementation of a finite element solution to the steady-state photon diffusion equation.

This work was supported by the following NIH grants: PD1 HL123271, R01 HL103428, and R01 HL111649.

Biography

Patrick M Boyle, PhD is an Assistant Research Scientist at the Institute for Computational Medicine at Johns Hopkins University. His current research focuses on the development and application of cutting edge multiscale cardiac electrophysiology models. Using this “virtual heart” framework, he conducts realistic simulations to explore optogenetics-based therapy of cardiac arrhythmias, devise patient-specific treatment strategies for persistent atrial fibrillation, probe structure-function relationships relevant to heart function, and quantify wavefront propagation robustness (i.e., “safety factor”) in electrically excitable tissue.

Thomas V Karathanos, MEng is a pre-doctoral student in Biomedical Engineering at Johns Hopkins University. He is interested in using multiscale computational modeling to study the electrophysiological effects of exogenous gene delivery in heart cells and tissue. His current research project explores the use of optogenetics as an alternative method for defibrillation.

Emilia Entcheva, PhD is a Professor in the Department of Biomedical Engineering at Stony Brook University, where she directs the Cardiac Optogenetics & Optical Imaging Laboratory. Her current research interests focus on the development of new optical modalities for actuation and sensing of the electromechanical function in cardiac cells and tissues. Her research team uses design concepts from electrical, optical, mechanical, and chemical engineering to create the enabling technology for their studies.

Natalia A Trayanova, PhD is the Murray B Sachs Professor of Biomedical Engineering and Medicine at Johns Hopkins University. She directs the Computational Cardiology Laboratory at the Institute for Computational Medicine. She is a Fellow of the Heart Rhythm Society, the American Heart Association, the Biomedical Engineering Society, and the American Institute for Medical and Biological Engineering. The research in Dr. Trayanova's Computational Cardiology Laboratory is focused on understanding pathological electrophysiological and electromechanical behavior of the heart, with emphasis on mechanisms for cardiac arrhythmogenesis and pump dysfunction, and the improvement of the clinical therapies of defibrillation, atrial and ventricular ablation, and cardiac resynchronization therapy using a personalized approach.

References

1. Entcheva E. Cardiac optogenetics. Am J Physiol Heart Circ Physiol. 2013; 304(9):H1179–91. [PubMed: 23457014]
2. Boyle PM, Karathanos TV, Trayanova NA. “Beauty is a light in the heart”: The transformative potential of optogenetics for clinical applications in cardiovascular medicine. Trends in Cardiovascular Medicine(0).
3. Nagel G, Szellas T, Huhn W, Kateriya S, Adeishvili N, Berthold P, et al. Channelrhodopsin-2, a directly light-gated cation-selective membrane channel. Proc Natl Acad Sci U S A. 2003; 100(24): 13940–5. [PubMed: 14615590]
4. Boyden ES, Zhang F, Bamberg E, Nagel G, Deisseroth K. Millisecond-timescale, genetically targeted optical control of neural activity. Nat Neurosci. 2005; 8(9):1263–8. [PubMed: 16116447]
5. Zhang F, Wang LP, Boyden ES, Deisseroth K. Channelrhodopsin-2 and optical control of excitable cells. Nat Methods. 2006; 3(10):785–92. [PubMed: 16990810]

6. Han X, Boyden ES. Multiple-color optical activation, silencing, and desynchronization of neural activity, with single-spike temporal resolution. PLoS One. 2007; 2(3):e299. [PubMed: 17375185]
7. Chow BY, Han X, Dobry AS, Qian X, Chuong AS, Li M, et al. High-performance genetically targetable optical neural silencing by light-driven proton pumps. Nature. 2010; 463(7277):98–102. [PubMed: 20054397]
8. Gradinaru V, Zhang F, Ramakrishnan C, Mattis J, Prakash R, Diester I, et al. Molecular and cellular approaches for diversifying and extending optogenetics. Cell. 2010; 141(1):154–65. [PubMed: 20303157]
9. Bruegmann T, Malan D, Hesse M, Beiert T, Fuegemann CJ, Fleischmann BK, et al. Optogenetic control of heart muscle in vitro and in vivo. Nat Methods. 2010; 7(11):897–900. [PubMed: 20881965]
10. Jia Z, Valiunas V, Lu Z, Bien H, Liu H, Wang HZ, et al. Stimulating cardiac muscle by light: cardiac optogenetics by cell delivery. Circ Arrhythm Electrophysiol. 2011; 4(5):753–60. [PubMed: 21828312]
11. Nussinovitch U, Shinnawi R, Gepstein L. Modulation of cardiac tissue electrophysiological properties with light-sensitive proteins. Cardiovasc Res. 2014; 102(1):176–87. [PubMed: 24518144]
12. Arrenberg AB, Stainier DY, Baier H, Huisken J. Optogenetic control of cardiac function. Science. 2010; 330(6006):971–4. [PubMed: 21071670]
13. Vogt CC, Bruegmann T, Malan D, Ottersbach A, Roell W, Fleischmann BK, et al. Systemic gene transfer enables optogenetic pacing of mouse hearts. Cardiovasc Res. 2015; 106(2):338–43. [PubMed: 25587047]
14. Boyle PM, Entcheva E, Trayanova NA. See the light: can optogenetics restore healthy heartbeats? And, if it can, is it really worth the effort? Expert Rev Cardiovasc Ther. 2014; 12(1):17–20. [PubMed: 24308809]
15. Ambrosi CM, Klimas A, Yu J, Entcheva E. Cardiac applications of optogenetics. Prog Biophys Mol Biol. 2014; 115(2-3):294–304. [PubMed: 25035999]
16. Rudy Y, Ackerman MJ, Bers DM, Clancy CE, Houser SR, London B, et al. Systems approach to understanding electromechanical activity in the human heart: a national heart, lung, and blood institute workshop summary. Circulation. 2008; 118(11):1202–11. [PubMed: 18779456]
17. Trayanova NA, Rice JJ. Cardiac electromechanical models: from cell to organ. Front Physiol. 2011; 2:43. [PubMed: 21886622]
18. Trayanova NA, O'Hara T, Bayer JD, Boyle PM, McDowell KS, Constantino J, et al. Computational cardiology: how computer simulations could be used to develop new therapies and advance existing ones. Europace. 2012; 14(Suppl 5):v82–v9. [PubMed: 23104919]
19. Trayanova NA, Boyle PM. Advances in modeling ventricular arrhythmias: from mechanisms to the clinic. Wiley Interdiscip Rev Syst Biol Med. 2014; 6(2):209–24. [PubMed: 24375958]
20. Arevalo H, Rodriguez B, Trayanova N. Arrhythmogenesis in the heart: Multiscale modeling of the effects of defibrillation shocks and the role of electrophysiological heterogeneity. Chaos. 2007; 17(1):015103. [PubMed: 17411260]
21. Moreno JD, Zhu ZI, Yang PC, Bankston JR, Jeng MT, Kang C, et al. A computational model to predict the effects of class I anti-arrhythmic drugs on ventricular rhythms. Sci Transl Med. 2011; 3(98):98ra83.
22. McDowell KS, Arevalo HJ, Maleckar MM, Trayanova NA. Susceptibility to arrhythmia in the infarcted heart depends on myofibroblast density. Biophys J. 2011; 101(6):1307–15. [PubMed: 21943411]
23. Bordas R, Gillow K, Lou Q, Efimov IR, Gavaghan D, Kohl P, et al. Rabbit-specific ventricular model of cardiac electrophysiological function including specialized conduction system. Prog Biophys Mol Biol. 2011; 107(1):90–100. [PubMed: 21672547]
24. Boyle PM, Veenhuyzen GD, Vigmond EJ. Fusion during entrainment of orthodromic reciprocating tachycardia is enhanced for basal pacing sites but diminished when pacing near Purkinje system end points. Heart Rhythm. 2013; 10(3):444–51. [PubMed: 23207137]

25. Boyle PM, Masse S, Nanthakumar K, Vigmond EJ. Transmural IK(ATP) heterogeneity as a determinant of activation rate gradient during early ventricular fibrillation: mechanistic insights from rabbit ventricular models. Heart Rhythm. 2013; 10(11):1710–7. [PubMed: 23948344]
26. Deo M, Ruan Y, Pandit SV, Shah K, Berenfeld O, Blaufox A, et al. KCNJ2 mutation in short QT syndrome 3 results in atrial fibrillation and ventricular proarrhythmia. Proc Natl Acad Sci U S A. 2013; 110(11):4291–6. [PubMed: 23440193]
27. Boyle PM, Park CJ, Arevalo HJ, Vigmond EJ, Trayanova NA. Sodium current reduction unmasks a structure-dependent substrate for arrhythmogenesis in the normal ventricles. PLoS One. 2014; 9(1):e86947. [PubMed: 24489810]
28. Chang KC, Bayer JD, Trayanova NA. Disrupted calcium release as a mechanism for atrial alternans associated with human atrial fibrillation. PLoS Comput Biol. 2014; 10(12):e1004011. [PubMed: 25501557]
29. Sadrieh A, Domanski L, Pitt-Francis J, Mann SA, Hodkinson EC, Ng CA, et al. Multiscale cardiac modelling reveals the origins of notched T waves in long QT syndrome type 2. Nat Commun. 2014; 5:5069. [PubMed: 25254353]
30. Niederer SA, Smith NP. The role of the Frank-Starling law in the transduction of cellular work to whole organ pump function: a computational modeling analysis. PLoS Comput Biol. 2009; 5(4):e1000371. [PubMed: 19390615]
31. Gurev V, Constantino J, Rice JJ, Trayanova NA. Distribution of electromechanical delay in the heart: insights from a three-dimensional electromechanical model. Biophys J. 2010; 99(3):745–54. [PubMed: 20682251]
32. Hu Y, Gurev V, Constantino J, Trayanova N. Efficient preloading of the ventricles by a properly timed atrial contraction underlies stroke work improvement in the acute response to cardiac resynchronization therapy. Heart Rhythm. 2013; 10(12):1800–6. [PubMed: 23928177]
33. Hu Y, Gurev V, Constantino J, Trayanova N. Optimizing cardiac resynchronization therapy to minimize ATP consumption heterogeneity throughout the left ventricle: a simulation analysis using a canine heart failure model. Heart Rhythm. 2014; 11(6):1063–9. [PubMed: 24657430]
34. Tandri H, Weinberg SH, Chang KC, Zhu R, Trayanova NA, Tung L, et al. Reversible cardiac conduction block and defibrillation with high-frequency electric field. Sci Transl Med. 2011; 3(102):102ra96.
35. Rantner LJ, Tice BM, Trayanova NA. Terminating ventricular tachyarrhythmias using far-field low-voltage stimuli: mechanisms and delivery protocols. Heart Rhythm. 2013; 10(8):1209–17. [PubMed: 23628521]
36. Rantner LJ, Vadakkumpadan F, Spevak PJ, Crosson JE, Trayanova NA. Placement of implantable cardioverter defibrillators in paediatric and congenital heart defect patients: a pipeline for model generation and simulation prediction of optimal configurations. J Physiol. 2013; 591(Pt 17):4321–34. [PubMed: 23798492]
37. Vadakkumpadan F, Rantner LJ, Tice B, Boyle P, Prassl AJ, Vigmond E, et al. Image-based models of cardiac structure with applications in arrhythmia and defibrillation studies. J Electrocardiol. 2009; 42(2):157, e1–10. [PubMed: 19181330]
38. Lamata P, Niederer S, Nordsletten D, Barber DC, Roy I, Hose DR, et al. An accurate, fast and robust method to generate patient-specific cubic Hermite meshes. Med Image Anal. 2011; 15(6): 801–13. [PubMed: 21788150]
39. Niederer SA, Plank G, Chinchapatnam P, Ginks M, Lamata P, Rhode KS, et al. Length-dependent tension in the failing heart and the efficacy of cardiac resynchronization therapy. Cardiovasc Res. 2011; 89(2):336–43. [PubMed: 20952413]
40. Ashikaga H, Arevalo H, Vadakkumpadan F, Blake RC 3rd, Bayer JD, Nazarian S, et al. Feasibility of image-based simulation to estimate ablation target in human ventricular arrhythmia. Heart Rhythm. 2013; 10(8):1109–16. [PubMed: 23608593]
41. Arevalo H, Plank G, Helm P, Halperin H, Trayanova N. Tachycardia in post-infarction hearts: insights from 3D image-based ventricular models. PLoS One. 2013; 8(7):e68872. [PubMed: 23844245]
42. Vadakkumpadan F, Trayanova N, Wu KC. Image-based left ventricular shape analysis for sudden cardiac death risk stratification. Heart Rhythm. 2014; 11(10):1693–700. [PubMed: 24854217]

43. Prakosa A, Malamas P, Zhang S, Pashakhanloo F, Arevalo H, Herzka DA, et al. Methodology for image-based reconstruction of ventricular geometry for patient-specific modeling of cardiac electrophysiology. Prog Biophys Mol Biol. 2014; 115(2-3):226–34. [PubMed: 25148771]
44. Boyle PM, Williams JC, Ambrosi CM, Entcheva E, Trayanova NA. A comprehensive multiscale framework for simulating optogenetics in the heart. Nat Commun. 2013; 4:2370. [PubMed: 23982300]
45. Bamann C, Kirsch T, Nagel G, Bamberg E. Spectral characteristics of the photocycle of channelrhodopsin-2 and its implication for channel function. J Mol Biol. 2008; 375(3):686–94. [PubMed: 18037436]
46. Hegemann P, Ehlenbeck S, Gradmann D. Multiple photocycles of channelrhodopsin. Biophys J. 2005; 89(6):3911–8. [PubMed: 16169986]
47. Nikolic K, Grossman N, Grubb MS, Burrone J, Toumazou C, Degenaar P. Photocycles of channelrhodopsin-2. Photochem Photobiol. 2009; 85(1):400–11. [PubMed: 19161406]
48. Williams JC, Xu J, Lu Z, Klimas A, Chen X, Ambrosi CM, et al. Computational optogenetics: empirically-derived voltage-and light-sensitive channelrhodopsin-2 model. PLoS Comput Biol. 2013; 9(9):e1003220–e. [PubMed: 24068903]
49. Entcheva E, Williams JC. Channelrhodopsin2 Current During the Action Potential: “Optical AP Clamp” and Approximation. Sci Rep. 2014; 4:5838. [PubMed: 25060859]
50. ten Tusscher KHWJ, Panfilov AV. Alternans and spiral breakup in a human ventricular tissue model. Am J Physiol Heart Circ Physiol. 2006; 291(3):H1088–H100. [PubMed: 16565318]
51. Park SA, Lee SR, Tung L, Yue DT. Optical mapping of optogenetically shaped cardiac action potentials. Sci Rep. 2014; 4:6125. [PubMed: 25135113]
52. Nikolic K, Jarvis S, Grossman N, Schultz S. Computational models of optogenetic tools for controlling neural circuits with light. Conf Proc IEEE Eng Med Biol Soc. 2013; 2013:5934–7. [PubMed: 24111090]
53. Chow BY, Han X, Boyden ES. Genetically encoded molecular tools for light-driven silencing of targeted neurons. Prog Brain Res. 2012; 196:49–61. [PubMed: 22341320]
54. Kleinlogel S, Feldbauer K, Dempski RE, Fotis H, Wood PG, Bamann C, et al. Ultra light-sensitive and fast neuronal activation with the Ca(2)+-permeable channelrhodopsin CatCh. Nat Neurosci. 2011; 14(4):513–8. [PubMed: 21399632]
55. Bingen BO, Engels MC, Schalij MJ, Jangsangthong W, Neshati Z, Feola I, et al. Light-induced termination of spiral wave arrhythmias by optogenetic engineering of atrial cardiomyocytes. Cardiovasc Res. 2014; 104(1):194–205. [PubMed: 25082848]
56. Klapoetke NC, Murata Y, Kim SS, Pulver SR, Birdsey-Benson A, Cho YK, et al. Independent optical excitation of distinct neural populations. Nat Methods. 2014; 11(3):338–46. [PubMed: 24509633]
57. Lin JY, Knutsen PM, Muller A, Kleinfeld D, Tsien RY. ReaChR: a red-shifted variant of channelrhodopsin enables deep transcranial optogenetic excitation. Nat Neurosci. 2013; 16(10): 1499–508. [PubMed: 23995068]
58. Williams JC, Xu J, Lu Z, Klimas A, Chen X, Ambrosi CM, et al. Computational optogenetics: empirically-derived voltage-and light-sensitive channelrhodopsin-2 model. PLoS Comput Biol. 2013; 9(9):e1003220. [PubMed: 24068903]
59. Ambrosi CM, Entcheva E. Optogenetic Control of Cardiomyocytes via Viral Delivery. Methods Mol Biol. 2014; 1181:215–28. [PubMed: 25070340]
60. Hofmann B, Maybeck V, Eick S, Meffert S, Ingebrandt S, Wood P, et al. Light induced stimulation and delay of cardiac activity. Lab Chip. 2010; 10(19):2588–96. [PubMed: 20689860]
61. Abilez OJ, Wong J, Prakash R, Deisseroth K, Zarins CK, Kuhl E. Multiscale computational models for optogenetic control of cardiac function. Biophys J. 2011; 101(6):1326–34. [PubMed: 21943413]
62. Beiert T, Bruegmann T, Sasse P. Optogenetic activation of Gq signalling modulates pacemaker activity of cardiomyocytes. Cardiovasc Res. 2014; 102(3):507–16. [PubMed: 24576953]
63. Ambrosi CM, Klimas A, Yu J, Entcheva E. Cardiac applications of optogenetics. Prog Biophys Mol Biol. 2014

64. Rosen AB, Kelly DJ, Schuldt AJT, Lu J, Potapova IA, Doronin SV, et al. Finding fluorescent needles in the cardiac haystack: tracking human mesenchymal stem cells labeled with quantum dots for quantitative in vivo three-dimensional fluorescence analysis. Stem Cells. 2007; 25(8): 2128–38. [PubMed: 17495112]

65. Prasad K-MR, Smith RS, Xu Y, French BA. A single direct injection into the left ventricular wall of an adeno-associated virus 9 (AAV9) vector expressing extracellular superoxide dismutase from the cardiac troponin-T promoter protects mice against myocardial infarction. J Gene Med. 2011; 13(6):333–41. [PubMed: 21674736]

66. Prasad KM, Xu Y, Yang Z, Acton ST, French BA. Robust cardiomyocyte-specific gene expression following systemic injection of AAV: in vivo gene delivery follows a Poisson distribution. Gene Ther. 2011; 18(1):43–52. [PubMed: 20703310]

67. Comtois P, Nattel S. Interactions between cardiac fibrosis spatial pattern and ionic remodeling on electrical wave propagation. 2011 Annual International Conference of the Ieee Engineering in Medicine and Biology Society (Embc). 2011; 2011:4669–72.

68. McDowell KS, Vadakkumpadan F, Blake R, Blauer J, Plank G, Macleod RS, et al. Methodology for patient-specific modeling of atrial fibrosis as a substrate for atrial fibrillation. J Electrocardiol. 2012

69. McDowell KS, Vadakkumpadan F, Blake R, Blauer J, Plank G, Macleod RS, et al. Mechanistic inquiry into the role of tissue remodeling in fibrotic lesions in human atrial fibrillation. Biophys J. 2013; 104(12):2764–73. [PubMed: 23790385]

70. Moran PA. Notes on continuous stochastic phenomena. Biometrika. 1950; 37(1-2):17–23. [PubMed: 15420245]

71. Trayanova NA. Mathematical approaches to understanding and imaging atrial fibrillation: significance for mechanisms and management. Circ Res. 2014; 114(9):1516–31. [PubMed: 24763468]

72. Trayanova NA. Whole-heart modeling: applications to cardiac electrophysiology and electromechanics. Circ Res. 2011; 108(1):113–28. [PubMed: 21212393]

73. Klimas A, Entcheva E. Toward microendoscopy-inspired cardiac optogenetics in vivo: technical overview and perspective. J Biomed Opt. 2014; 19(8):080701. [PubMed: 25117076]

74. Kim TI, McCall JG, Jung YH, Huang X, Siuda ER, Li Y, et al. Injectable, cellular-scale optoelectronics with applications for wireless optogenetics. Science. 2013; 340(6129):211–6. [PubMed: 23580530]

75. Xu L, Gutbrod SR, Bonifas AP, Su Y, Sulkin MS, Lu N, et al. 3D multifunctional integumentary membranes for spatiotemporal cardiac measurements and stimulation across the entire epicardium. Nat Commun. 2014; 5:3329. [PubMed: 24569383]

76. Baxter WT, Mironov SF, Zaitsev AV, Jalife J, Pertsov AM. Visualizing excitation waves inside cardiac muscle using transillumination. Biophys J. 2001; 80(1):516–30. [PubMed: 11159422]

77. Weissleder R, Ntziachristos V. Shedding light onto live molecular targets. Nat Med. 2003; 9(1): 123–8. [PubMed: 12514725]

78. Bishop MJ, Rodriguez B, Eason J, Whiteley JP, Trayanova N, Gavaghan DJ. Synthesis of voltage-sensitive optical signals: application to panoramic optical mapping. Biophys J. 2006; 90(8):2938–45. [PubMed: 16443665]

79. Bishop MJ, Plank G. Simulating Photon Scattering Effects in Structurally Detailed Ventricular Models Using a Monte Carlo Approach. Frontiers in Physiology. 2014:5. [PubMed: 24478718]

80. Ding L, Splinter R, Knisley SB. Quantifying spatial localization of optical mapping using Monte Carlo simulations. IEEE Trans Biomed Eng. 2001; 48(10):1098–107. [PubMed: 11585033]

81. Courtemanche M, Ramirez RJ, Nattel S. Ionic mechanisms underlying human atrial action potential properties: insights from a mathematical model. Am J Physiol. 1998; 275(1 Pt 2):301–21.

82. Sampson KJ, Iyer V, Marks AR, Kass RS. A computational model of Purkinje fibre single cell electrophysiology: implications for the long QT syndrome. J Physiol. 2010; 588(Pt 14):2643–55. [PubMed: 20498233]

83. Williams JC, Entcheva E. Optogenetic vs. Electrical Stimulation of Human Cardiomyocytes: Modeling Insights. Biophys J. 2015 in press.

84. Boyle PM, Deo M, Plank G, Vigmond EJ. Purkinje-mediated effects in the response of quiescent ventricles to defibrillation shocks. Ann Biomed Eng. 2010; 38(2):456–68. [PubMed: 19876737]

85. Wong J, Abilez OJ, Kuhl E. Computational Optogenetics: A Novel Continuum Framework for the Photoelectrochemistry of Living Systems. J Mech Phys Solids. 2012; 60(6):1158–78. [PubMed: 22773861]

86. Provost J, Gurev V, Trayanova N, Konofagou EE. Mapping of cardiac electrical activation with electromechanical wave imaging: an in silico-in vivo reciprocity study. Heart Rhythm. 2011; 8(5): 752–9. [PubMed: 21185403]

87. Gurev V, Lee T, Constantino J, Arevalo H, Trayanova NA. Models of cardiac electromechanics based on individual hearts imaging data: image-based electromechanical models of the heart. Biomech Model Mechanobiol. 2011; 10(3):295–306. [PubMed: 20589408]

88. Karathanos TV, Boyle PM, Trayanova NA. Optogenetics-Enabled Dynamic Modulation of Action Potential Duration in Atrial Tissue: Feasibility of a Novel Therapeutic Approach. Europace. 2014 in press.

89. Karathanos TV, Boyle PM, Trayanova NA. Optogenetics-enabled dynamic modulation of action potential duration in atrial tissue: feasibility of a novel therapeutic approach. Europace. 2014; 16(Suppl 4):iv69–iv76. [PubMed: 25362173]

90. McDowell KS, Vadakkumpadan F, Blake R, Blauer J, Plank G, MacLeod RS, et al. Methodology for patient-specific modeling of atrial fibrosis as a substrate for atrial fibrillation. J Electrocardiol. 2012; 45(6):640–5. [PubMed: 22999492]

Highlights

- In Part 1, we discuss state-of-the-art methods used to model cardiac optogenetics
- Required techniques at the protein, cell, tissue, and organ scales are summarized
- A novel exploration of optogenetic cardiac action potential silencing is included
- In Part 2, we review findings that have emerged from cardiac optogenetics modeling
- Simulations will help assess the efficacy of potential clinical applications

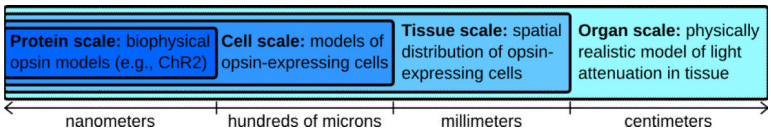

Figure 1.

Schematic showing new methodologies that must be integrated with the existing approach to multiscale cardiac modeling. Changes required at four discrete spatial scales are highlighted.

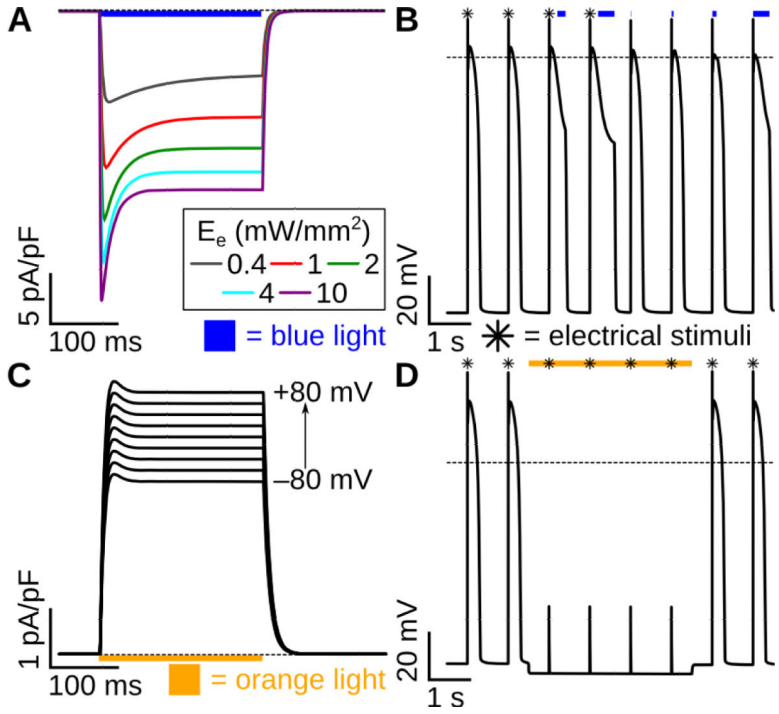

Figure 2.

Simulated response to optogenetics-based stimulation of opsin-expressing human cardiomyocytes. (A) ChR2-mediated photocurrent (I_{ChR2}) in response to 200 ms of blue-light illumination with a range of irradiance (E_e) levels; I_{ChR2} is modeled as described by Williams et al. (48) and incorporated in a human ventricular myocyte (50) clamped to V_m = –80 mV. (B) Result of electrical and optogenetics-based stimulation in the human ventricular myocyte. Both light-based action potential (AP) prolongation (beats 3 and 4) and purely light-elicited APs (beats 5 to 8) are shown. Blue light pulses had E_e = 10mW/mm^2. (C) NpHR-mediated photocurrent (I_{NpHR} in response to 200 ms pulses of orange light (E_e = 1.4 mW/mm2) in ventricular myocytes clamped to a range of V_m values. The formulation used to model I_{NpHR} is provided Table 1. (D) Optogenetics-based "silencing" of electrical stimuli that would otherwise have induced APs. The orange light pulse had E_e = 1.4 mW/mm^2. Electrical stimuli were transmembrane current pulses (strength: 32.4 μA/cm^2, duration: 1 ms); NpHR-based silencing failed when stronger and/or long-lasting electrical stimuli needed to be countered by light.

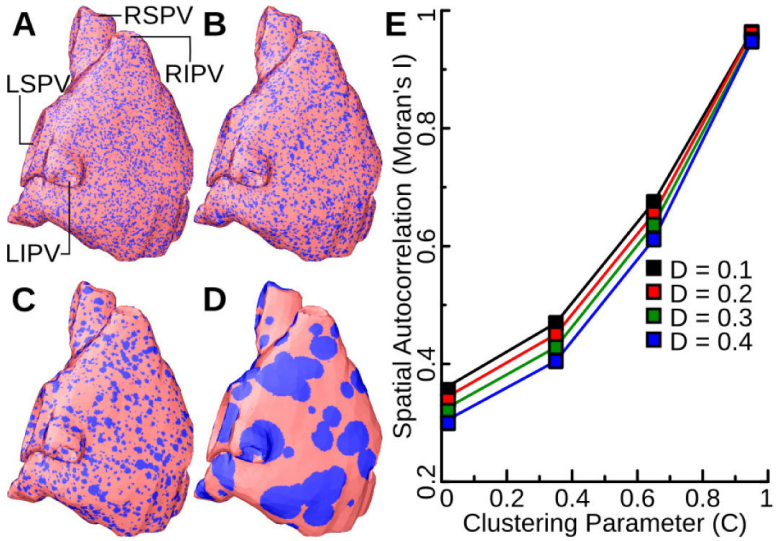

Figure 3.

Simulated distribution of opsin-expressing cells in an image-based human left atrial model (68,69). (A-D) Patterns resulting from applying the stochastic distribution algorithm described in the text with D = 0.4 and C = 0, 0.35, 0.65, and 0.95. Blue and pink regions represent opsin-expressed and non-modified tissue, respectively. Anatomical labels in A indicate the left and right superior and inferior pulmonary veins. (E) Relationship between Moran's I (70), a spatial metric quantifying clustering, and the C parameter of the distribution algorithm for different values of D.

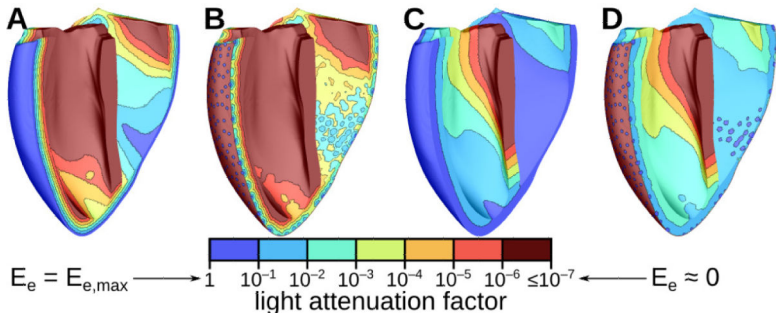

Figure 4.

Ventricular distribution of irradiance (E_e) values resulting from epicardial optical stimulation. (A-B) Uniform and multi-point illumination, respectively, with blue light (λ = 488 nm) appropriate for excitation of ChR2. For this wavelength of light, the penetration depth in cardiac tissue is approximately 588 μm (80). Note that light attenuation is plotted on a logarithmic scale. (C-D) Same as A-B but for illumination with red light (λ = 669 nm), for which the penetration depth is 1.84 mm (80), which would be appropriate for illumination of certain red-shifted ChR2 variants (e.g., Chrimson (56) or ReaChR (57)).

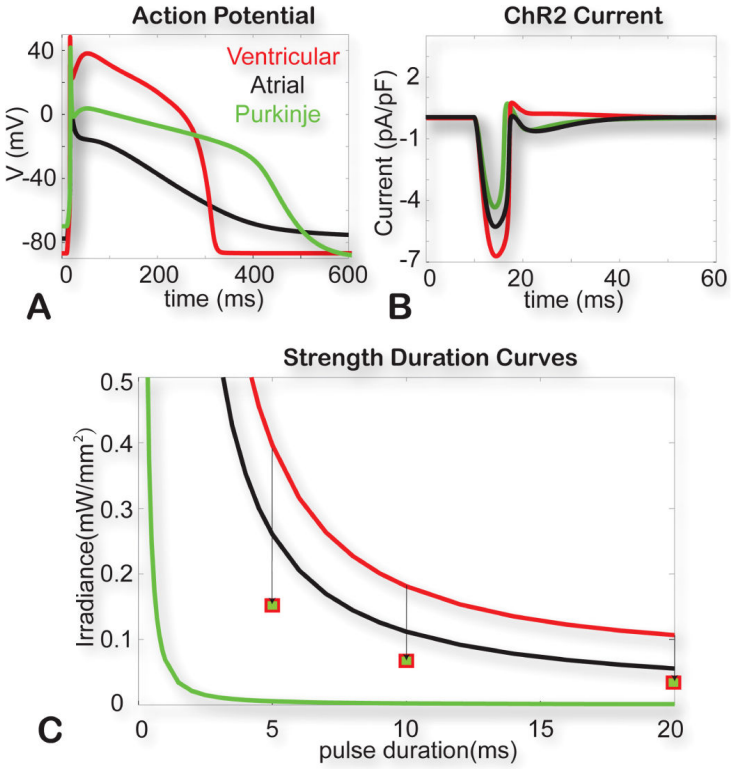

Figure 5.

Comparison of ChR2 photocurrent required for optogenetics-based excitation in models of different cardiac cell types. (A) Simulated action potentials (APs) induced by optogenetics-based stimulation (E_e = 0.5 mW/mm^2 over 10 ms) of ChR2-expressing cardiac cells from different regions of the heart (ventricular (50), atrial (81), and Purkinje fiber (82)). (B) Underlying light-sensitive current for APs shown in A. (C) Strength-duration (SD) relationships for optogenetics-based stimulation of different cardiac cell types; squares indicate the effect on the ventricular SD curve when the formulation for inward-rectifying potassium current (I_{K1}) in that model was replaced with the version from the Purkinje fiber model. Reproduced with permission from Williams et al. (48).

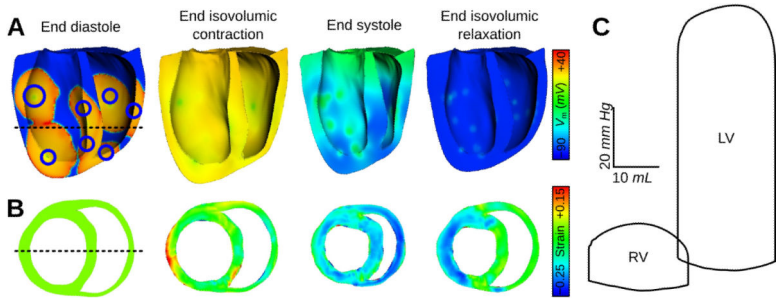

Figure 6.

Contraction of canine ventricular electromechanical model in response to simultaneous optogenetics-based pacing from ten locations corresponding to Purkinje system endpoints. (A-B) Spatial maps of membrane voltage (V_m) and strain (measured with respect to end diastolic state) at different phases of the cardiac cycle. Optical stimuli (E_e = 12.8 mW/mm^2, 10 ms duration) were applied at 10 distinct ventricular sites located near Purkinje system endpoints. (C) Left and right ventricular (LV, RV) pressure-volume loops for the photo-evoked response, which closely matched those corresponding to normal sinus rhythm (cross-correlation coefficient γ = 0.9). Reproduced with permission from Boyle et al. (44).

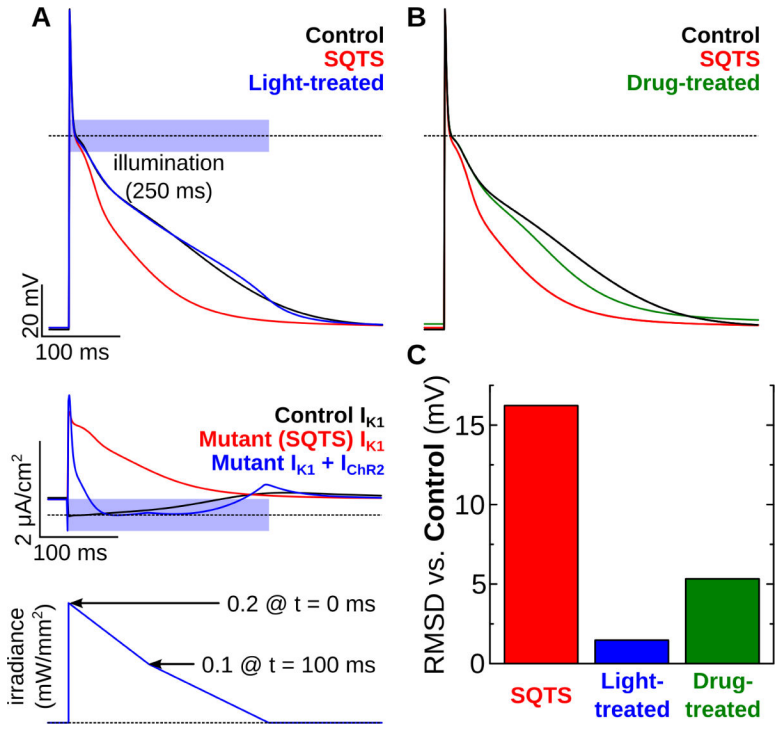

Figure 7.

Optogenetics-based dynamic modulation of action potential duration in atrial myocytes. (A) Comparison of atrial action potentials (APs) under three model conditions: normal (control), diseased (SQTS; short QT syndrome caused by a KCNJ2 mutation (26)), and SQTS with optogenetics-based stimulation to modulate (lengthen) AP duration. Selected ionic currents and optical stimulus pulse features are shown in the middle and lower panels, respectively. (B) Same as top panel of A but with SQTS treated via chloroquine. (C) Quantitative comparison between control APs and diseased/treated APs for cases in A and B; smaller values indicate better matches. Reproduced with permission from Karathanos et al. (88).

Table 1

Equations and parameters for NpHR opsin model, based on the formulation used by Nikolic et al. (52). Rate coefficients were obtained via private correspondence with Professor Konstantin Nikolic. Other parameters (membrane voltage-sensitive scaling function ($f(V_m)$), NpHR conductance per unit area (g_{NpHR}), and sub-threshold irradiance (E_{e0})) were calibrated to achieve a good match between steady-state I_{NpHR} values and experimentally measured currents in NpHR-expressing myocytes illuminated at 1.4 mW/mm^2 (compare Fig. 2C with Figs. 1b,d in the study by Park et al. (51)).

Category	Parameter	Value / Equation	Units
Opsin Model	NpHR photocurrent	$I_{NpHR} = g_{NpHR} \times f(V_m) \times O$	μA/ cm^2
	NpHR conductance	$g_{NpHR} = 1$	mS/cm^2
	V_m-dependent scaling function	$f(V_m) = 75.2 + 0.193 \times V_m$	mV
	Sub-threshold irradiance	$E_{e0} = 0.00014$	mW/mm^2
State Differentials	O (initial value = 0)	$dO/dt = C \times \alpha_1 - O \times \alpha_2$	
	C (initial value = 1)	$dC/dt = I \times \alpha_3 - C \times \alpha_1$	
	I (initial value = 0)	$dI/dt = O \times \alpha_2 - I \times \alpha_3$	
Rate Coefficients	Opening (C to O)	$\alpha_1 = 0.002 \times E_e/E_{e0}$	ms^{-1}
	Inactivation (O to I)	$\alpha_2 = 0.1$	ms^{-1}
	Recovery (I to C)	$\alpha_3 = \alpha_{3D} + \alpha_{3L}$	ms^{-1}
	Light-insensitive recovery	$\alpha_{3D} = 0.1$	ms^{-1}
	Light-sensitive recovery	$\alpha_{3L} = 0.02 \times \log_{10}(E_e/E_{e0})$	ms^{-1}